Clinical & Translational Immunology

Australian and New Zealand Society for Immunology Inc.

Clinical & Translational Immunology 2022; e1402. doi: 10.1002/cti2.1402
www.wileyonlinelibrary.com/journal/cti

ORIGINAL ARTICLE

Detailed bladder cancer immunoprofiling reveals new clues for immunotherapeutic strategies

Nicole Viveiros[1], Bianca CT Flores[1], João Lobo[1,2,3], Cláudia Martins-Lima[1,4], Mariana Cantante[1,2], Paula Lopes[1,2], Cecilia Deantonio[5], Cintia Palu[5], Richard CA Sainson[5], Rui Henrique[1,2,3] & Carmen Jerónimo[1,3]

[1]Cancer Biology and Epigenetics Group, Research Center of IPO Porto (CI-IPOP)/RISE@CI-IPOP (Health Research Network), Portuguese Oncology Institute of Porto (IPO Porto)/Porto Comprehensive Cancer Center (Porto.CCC), Porto, Portugal
[2]Department of Pathology, Portuguese Oncology Institute of Porto (IPO Porto), Porto, Portugal
[3]Department of Pathology and Molecular Immunology, School of Medicine and Biomedical Sciences– University of Porto (ICBAS-UP), Porto, Portugal
[4]Department of Precision Medicine, University of Campania "Luigi Vanvitelli", Naples, Italy
[5]Kymab, a Sanofi Company, Cambridge, UK

Correspondence
C Jerónimo and R Henrique, Portuguese Oncology Institute of Porto (IPOP), R. Dr António Bernardino de Almeida, 4200-072, Porto, Portugal.
E-mails:
carmenjeronimo@ipoporto.min-saude.pt (CJ);
henrique@ipoporto.min-saude.pt (RH)

Received 12 January 2022;
Revised 22 May 2022;
Accepted 17 June 2022

doi: 10.1002/cti2.1402

Clinical & Translational Immunology
2022; **11**: e1402

Abstract

Objectives. Bladder cancer (BlCa) is the tenth most frequent malignancy worldwide and the costliest to treat and monitor. Muscle-invasive BlCa (MIBC) has a dismal prognosis, entailing the need for alternative therapies for the standard radical cystectomy. Checkpoint blockade immunotherapy has been approved for high-grade non-muscle-invasive BlCa (HG NMIBC) and metastatic disease, but its effectiveness in localised MIBC remains under scrutiny. Herein, we sought to characterise and compare the immune infiltrate of HG NMIBC and MIBC samples, including ICOS expression, a targetable immune checkpoint associated with regulatory T cell(T_{regs})-mediated immunosuppression. **Methods.** Immunohistochemistry for CD83, CD20, CD68, CD163, CD3, CD8, CD4, FoxP3/ICOS and PD-L1 was performed in HG NMIBC and MIBC samples ($n = 206$), and positive staining was quantified in the peritumoral and/or intratumoral tissue compartments with QuPath imaging software. **Results.** $CD20^+$ B cells, $CD68^+$ and $CD163^+$ tumor-associated macrophages were significantly increased in MIBCs and associated with poor prognosis. In turn, higher infiltration of T cells was associated with prolonged survival, with exception of the $CD4^+$ helper subset. Intratumoral expression of CD3 and CD8 was independent prognostic factors for increased disease-free survival (DFS) in multivariable analysis. Remarkably, T_{regs} ($FoxP3^+/FoxP3^+ICOS^+$) were found differentially distributed between tissue compartments. PD-L1 immunoexpression independently predicted a shorter DFS and associated with higher infiltration of $FoxP3^+ICOS^+$ T_{regs}. **Conclusions.** Immune infiltrates of HG NMIBC and MIBC display significant differences that may help selecting patients for immunotherapies. Considering ICOS immunoexpression results, it might constitute a relevant

therapeutic target, eventually in combination with anti-PD-1/PD-L1 therapies, for certain BlCa patient subsets.

Keywords: bladder cancer, digital pathology, ICOS, immune infiltrate, muscle-invasive, non-muscle invasive

INTRODUCTION

Bladder cancer (BlCa) is the tenth most common malignancy worldwide, accounting for 573 278 new cases and 212 536 deaths in 2020.[1] The high recurrence and progression rates often raise the need for lifelong monitoring and care, endowing BlCa with the highest cost per patient of all cancer types.[2,3] Histologically, 90% of cases correspond to urothelial carcinoma,[4] and approximately 70–80% of patients are diagnosed with non-muscle invasive tumors (NMIBC) of which 50–70% end up recurring and 15–25% of the latter progress to muscle-invasive BlCa (MIBC).[4] MIBC has a substantial risk of metastatic dissemination (about 50%), with a dismal prognosis. Over the years, limited improvements in BlCa survival rates were recorded, especially for MIBC,[5] a scenario that has recently improved after approval of immune checkpoint inhibitors (ICIs)-based immunotherapy.

Immunotherapy relies on the activation of the host immune system to destroy cancer cells and has revolutionised the oncology field, improving patients' outcomes in multiple malignancies. ICIs have particularly attracted researchers, because of their ability to unleash an antitumor T-cell response, through blockage of inhibitory molecules expressed in the surface of T cells after excessive stimulation or their ligands, including cytotoxic T lymphocyte-associated molecule-4 (CTLA-4), programmed cell death receptor-1 (PD-1) and programmed cell death receptor-1 ligand (PD-L1).[6] Remarkably, over 6000 active clinical trials are testing the efficacy of immuno-oncology drugs, including ICIs and other immunomodulators.[7]

BlCa is known to be immunotherapy-responsive since the 1970s when Bacillus Calmette-Guérin intravesical instillations proved to reduce recurrence and progression rates.[8] Because of its efficacy, Bacillus Calmette-Guérin remains the standard of care therapy for intermediate- and high-risk NMIBC after endoscopic resection. Moreover, since 2016, five ICIs targeting the PD-1/PD-L1 axis have been approved by the Food and Drug Administration for BlCa management.[9] These agents were first indicated for the treatment of locally advanced/metastatic urothelial carcinoma, either as second-line therapy for cisplatin-refractory patients or as first-line treatment in PD-L1$^+$ tumors of patients ineligible for cisplatin-based therapy. In January 2020, pembrolizumab was also approved for Bacillus Calmette-Guérin-unresponsive high-risk NMIBC, stepping the foot outside the metastatic BlCa setting. Notwithstanding the clinical benefits provided by ICIs, no immunotherapeutic options are available for localised MIBC, yet. Indeed, first-line therapy and standard of care is radical cystectomy, a complex surgical procedure that substantially increases cancer-related morbidity, but still represents the best hypothesis for patients to achieve long-term survival. Cisplatin-based neoadjuvant chemotherapy may also be offered, as it has been shown to improve 5- and 10-year survival by 8% and 30–36%, respectively.[10,11] However, many patients are not eligible or sensitive to chemotherapy, and high rates of severe adverse events have been reported,[12] entailing the need for effective alternatives. Mounting evidence suggests that neoadjuvant immunotherapy may benefit patients with localised MIBC,[13,14] but further investigation is required to support this hypothesis.

Simultaneously, a rising number of new targets are under investigation to broaden the applicability and efficacy of existing ICIs, such as Inducible Co-Stimulator (ICOS) and its ligand, ICOS-L. Despite belonging to the B7/Cluster of Differentiation (CD)28 superfamily, similarly to Cytotoxic T lymphocyte-associated molecule-4 and PD-1, ICOS is a costimulatory molecule that enhances T cells function.[15,16] Thus, ICOS endures both anti- and pro-tumor activities, depending on the T-cell subpopulation.[17] The role of this immune checkpoint in cancer is not fully understood at present, but it seems to constitute a promising therapeutic target.

Herein, we aimed to characterise and compare the immune infiltrate of high-grade (HG) NMIBC and MIBC samples, looking for profiles which might anticipate response to systemic

immunotherapies. Thus, we quantitatively evaluated the expression of several immune markers, representative of distinct immune cell populations, as well as PD-L1, a known biomarker predictive of response to immunotherapy, and ICOS. Immunohistochemistry quantification was performed using QuPath, an innovative digital pathology software[18] that allows a more consistent, accurate and reproducible analysis.

RESULTS

Clinical and pathological data

Clinicopathological features of the BlCa patient cohort are depicted in Table 1. Two hundred and six patients with primary BlCa were included in this study, with a median age of 69 years old, from which approximately 80% were male patients. At diagnosis, 93 individuals exhibited HG NMIBC and 113 displayed MIBC. Patients' follow-up time ranged from 1 to 267 months, with an overall 49.0% cancer-related mortality rate.

Table 1. Clinical and pathological features of BlCa patients

Variables	Patient cohort (n = 206)
Age, years [median (range)]	69 (1891)
Gender	
Male (%)	162 (78.6)
Female (%)	44 (21.4)
Primary Tumor (T)	
HG NMIBC (≤ pT1), (%)	93 (45.1)
Tx (%)	7/93 (7.6)
Ta (%)	19/93 (20.4)
T1 (%)	67/93 (72.0)
MIBC (≥ pT2), (%)	113 (54.9)
Tx (%)	9/113 (8.0)
T2 (%)	51/113 (45.1)
T3 (%)	29/113 (25.7)
T4 (%)	24/113 (21.2)
Regional lymph nodes (*N*)	
Nx (%)	161 (78.1)
N0 (%)	41 (19.9)
N1 (%)	2 (1.0)
N2 (%)	2 (1.0)
N3 (%)	0 (0.0)
Distant metastasis (M)	
M0 (%)	199 (96.6)
M1 (%)	7 (3.4)
Treatment	
Intravesical	50
BCG (%)	18/50 (36.0)
Mitomycin (%)	32/50 (64.0)
Systemic Chemotherapy	36
Smoking history	
No (%)	80 (38.8)
Yes (%)	62 (30.1)
Unknown (%)	64 (31.1)
Vital status at last follow-up	
A-NED (%)	33 (16.0)
AWD (%)	2 (1.0)
D-NED (%)	69 (33.5)
DWD (%)	1 (0.5)
DFD (%)	101 (49.0)

A-NED, alive with no evidence of disease; AWD, alive with disease; BCG, Bacillus Calmette-Guérin; D-NED, died with no evidence of disease; DWD, died with disease; DFD, died from disease; HG NMIBC, high-grade non-muscle invasive bladder cancer; MIBC, muscle-invasive bladder cancer.

Characterisation of the immune tumor microenvironment

Dendritic cells (DCs)

Mature DCs ($CD83^+$) were not abundant in most tumors. In fact, CD83 expression was absent inside the tumor area of all analysed samples and, for that reason, just $CD83^+$ cells in the peritumoral stroma were considered. CD83 counts were similar in HG NMIBC and MIBC (Supplementary figure 1). No associations were established between CD83 immunoexpression and BlCa prognosis.

B lymphocytes

Similar to DCs, infiltration of B lymphocytes, assessed by CD20 immunostaining, was rarely observed inside tumors. Therefore, only peritumoral B cells were considered for the analysis. Of note, only one sample lacked this immune cell population. Herein, CD20 expression was significantly increased in MIBC than in HG NMIBC ($P < 0.0001$; Figure 1a and b). Furthermore, Kaplan–Meier analysis revealed a significant association between higher $CD20^+$ cells density and worse disease-specific survival (DSS; $P = 0.0136$; Figure 1c); although the same trend was observed for overall survival (OS) and disease-free survival (DFS), no statistical significance was achieved ($P = 0.0752$ and $P = 0.1694$, respectively; Supplementary figure 2a and b).

Importantly, higher CD20 levels were observed in BlCa samples from male individuals ($P = 0.0046$; Supplementary figure 2c). It should be noted that no gender-related differences were disclosed for the remaining immune markers.

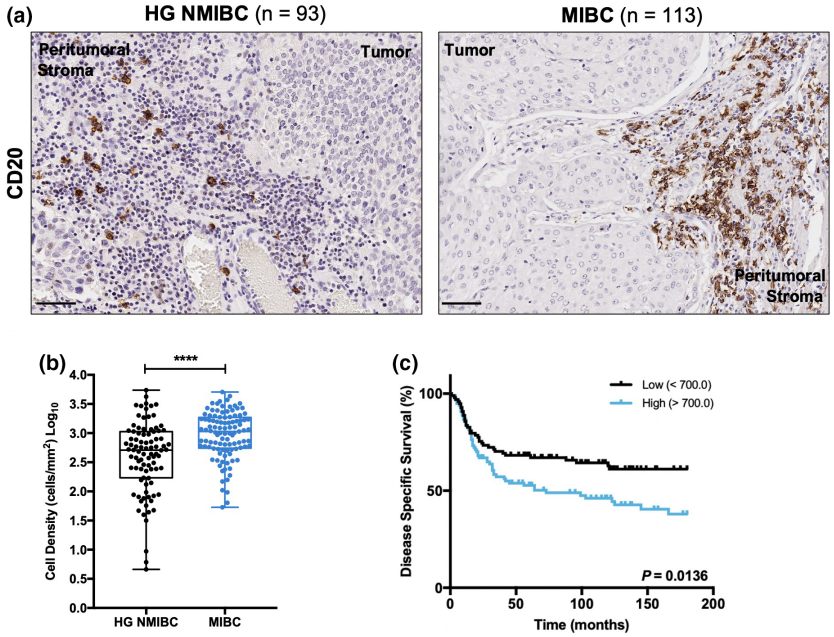

Figure 1. CD20 expression is associated with muscle invasion and poor prognosis. **(a)** Representative examples of CD20 staining in HG NMIBC and MIBC tissue specimens. Notice the absence of staining in the intratumoral area. Scale bar = 50 μm. **(b)** Distribution of $CD20^+$ cells density in HG NMIBC (n = 93) and MIBC (n = 113) samples. The number of positive cells per mm^2 was calculated with QuPath's *Positive Cell Detection* tool. *P*-values were calculated by the non-parametric Mann–Whitney *U*-test; ns $P > 0.05$, $*P < 0.05$, $**P < 0.01$, $***P < 0.001$, $****P < 0.0001$. **(c)** Kaplan–Meier estimates of DSS in BlCa patients stratified by CD20 expression. Dichotomisation into low and high expression was based on the median value. *P*-values were calculated by the log-rank test. HG NMIBC, high-grade non-muscle invasive bladder cancer; MIBC, muscle-invasive bladder cancer.

Tumor-associated macrophages (TAMs)

CD68 and CD163 immunoexpression was observed in all tumor samples, both peri- and intratumorally. Indeed, they exhibited the same expression pattern, with a highly increased positivity in patients with MIBC, both in peritumoral (CD68 – $P < 0.0001$; CD163 – $P = 0.0005$) and in intratumoral (CD68 and CD163 – $P < 0.0001$) regions (Figure 2). Moreover, CD68 and CD163 immunoexpression positively correlated in the evaluated compartments ($P < 0.0001$ for both; Spearman's rho = 0.7147 and 0.7211 for peritumoral and intratumoral TAMs, respectively), confirming that most TAMs exhibit an M2-like phenotype.

Higher counts of peritumoral $CD68^+$ TAMs were strongly associated with a poorer DSS ($P = 0.0370$; Figure 3a), while high levels of the intratumoral counterparts also negatively correlated with DSS ($P = 0.0082$) and OS ($P = 0.0204$; Figure 3b). Regarding $CD163^+$ TAMs, dense infiltration was also associated with worse DSS ($P = 0.0476$) and OS ($P = 0.0186$), but only when considering CD163 global expression (Figure 3c).

Additionally, intratumoral $CD163^+$ TAMs were augmented in the group of non-responders to intravesical chemotherapy (mitomycin; $P = 0.0121$; Figure 3d). Interestingly, no other immune cell subset was significantly associated, either negatively or positively, with response to this therapy.

T lymphocytes

Although T cells ($CD3^+$ immune cells) were abundant in most tumors, intratumoral expression was absent in 13 samples. Peritumoral $CD3^+$ cells were similarly expressed in HG NMIBC and MIBC. Nonetheless, a significant enrichment of intratumoral T cells was observed in MIBC ($P < 0.0001$; Supplementary figure 3a and b).

Importantly, higher counts of intratumoral T cells were associated with longer DFS ($P = 0.0393$; Supplementary figure 3c), whilst peritumoral T cells did not have a significant impact on OS, DSS

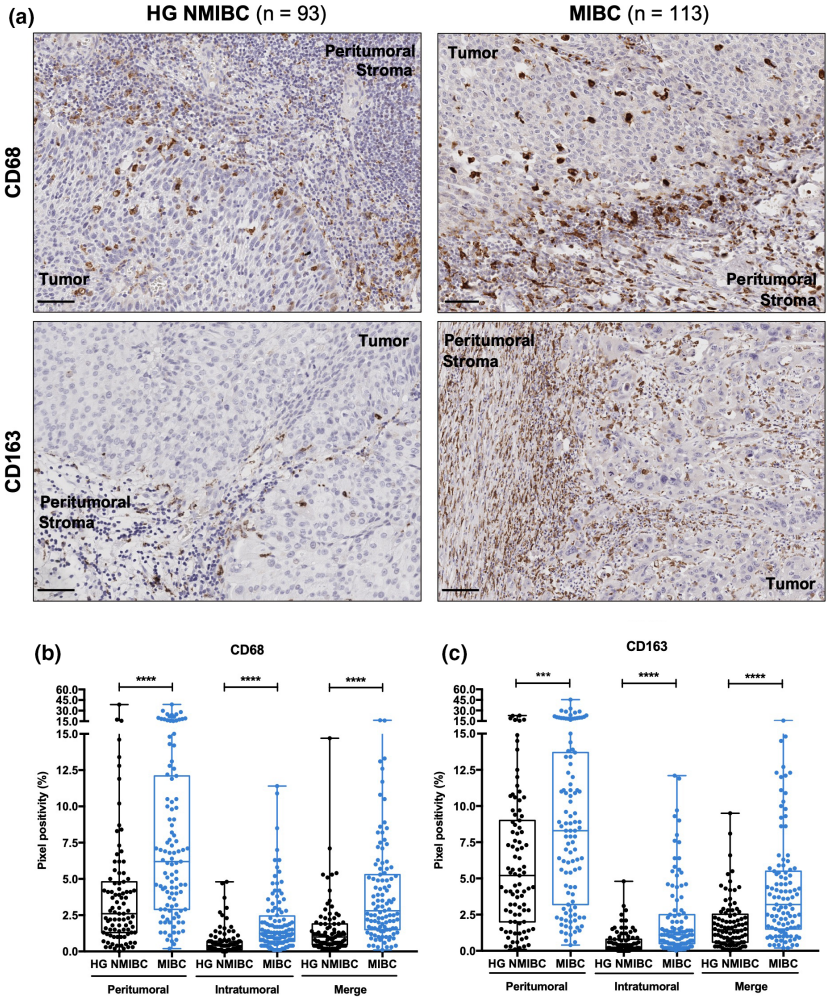

Figure 2. CD68 and CD163 expression is substantially higher in MIBC than in HG NMIBC. **(a)** Representative examples of CD68 and CD163 staining in HG NMIBC and MIBC tissue specimens. Notice the irregular, sometimes punctate staining pattern. Scale bar = 50 μm; Distribution of CD68 **(b)** and CD163 **(c)** positive percentage in HG NMIBC (n = 93) and MIBC (n = 113) samples. Pixel positivity was assessed with QuPath's *Pixel Classification* tool. 'Merge' refers to the whole-slide evaluation, considering peritumoral and intratumoral regions together. *P*-values were calculated by the non-parametric Mann–Whitney *U*-test; ns $P > 0.05$, *$P < 0.05$, **$P < 0.01$, ***$P < 0.001$, ****$P < 0.0001$. HG NMIBC, high-grade non-muscle invasive bladder cancer; MIBC, muscle-invasive bladder cancer.

or DFS ($P = 0.3271$, 0.2835 and 0.7427, respectively; Supplementary figure 4).

Further characterisation of the $CD3^+$ cells population was conducted, concerning $CD8^+$ cytotoxic T cells and $CD4^+$ helper T cells, with an emphasis on regulatory T cells (T_{regs}).

$CD8^+$ cytotoxic T cells

The predominance of $CD8^+$ cytotoxic T cells subset within the general T-cell population was verified in most tumors, with CD4/CD8 ratio > 1 in only five cases. CD8 immunoexpression varied similarly to CD3, in both in peri- and in intratumoral areas. Thus, intratumoral $CD8^+$ T-cell counts were higher in MIBC ($P < 0.0001$), but no differences were noticed at the *p*eritumoral level (Figure 4a and b).

Moreover, higher intratumoral CD8 expression was significantly associated with increased DFS ($P = 0.0150$; Figure 4c). The same trend was observed for peritumoral CD8, but without statistical significance ($P = 0.0713$; Figure 4d). In parallel, a stratified survival analysis was conducted separately for HG NMIBC and MIBC. Herein, intratumoral CD8 expression was significantly associated with longer DFS ($P = 0.0351$) and OS ($P = 0.0398$) in patients with MIBC, but not with HG NMIBC (Figure 4e).

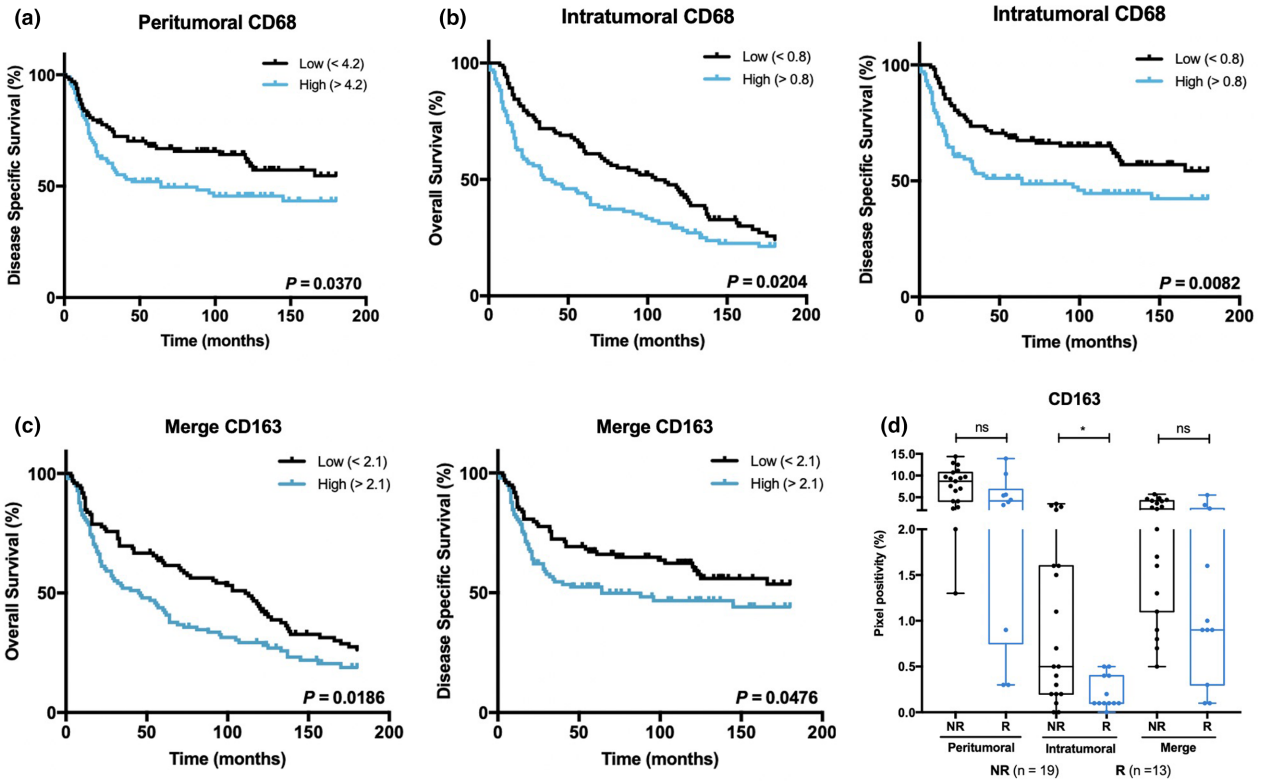

Figure 3. CD68$^+$ and CD163$^+$ TAMs correlate with prognosis and response to treatment of BlCa patients. Kaplan–Meier estimates of OS and/or DSS in BlCa patients stratified by peritumoral CD68 **(a)**, intratumoral CD68 **(b)** and merge CD163 expression **(c)**. Dichotomisation into low and high expression was based on the respective median values. *P*-values were calculated by the log-rank test. **(d)** Distribution of CD163 positive percentage, according to response to intravesical chemotherapy (mitomycin). 'Merge' refers to the whole-slide evaluation, considering peritumoral and intratumoral regions together. *P*-values were calculated by the non-parametric Mann–Whitney *U*-test; ns $P > 0.05$, $*P < 0.05$, $**P < 0.01$, $***P < 0.001$, $****P < 0.0001$. NR, non-responders; R, responders.

CD4$^+$ helper T cells

CD4$^+$ T cells were much less abundant than the CD8$^+$ subpopulation. Indeed, 31 cases completely lacked this T-cell subset. At the peritumoral level, CD4$^+$ T cells were more abundant in HG NMIBC ($P = 0.0052$); contrarily, increased CD4 immunoexpression was observed intratumorally in MIBC ($P = 0.0355$; Supplementary figure 5a and b).

Globally, no prognostic significance was initially assigned to this immune cell subset. Nonetheless, in patients with HG NMIBC, intratumoral CD4$^+$ cells were significantly associated with shorter DFS ($P = 0.0146$; Supplementary figure 5c).

Regulatory T cells and related immune checkpoints

Forkhead Box P3 (FoxP3)$^+$ T lymphocytes were found within most tumors, although more prevalent in the peritumoral region. Overall, this well-known T_{regs} marker was absent in 21 cases. Although no differences were apparent between HG NMIBC and MIBC, regarding FoxP3 immunoexpression, when patients were stratified based on pT stage, at the peritumoral level, this subpopulation was significantly diminished in pT3 and pT4 than in pTa-pT1 and pT2 tumors ($P = 0.0189$ and $P = 0.0470$, respectively). Intratumorally, FoxP3$^+$ cell counts were significantly higher in pT2 than in pTa-pT1 stages ($P = 0.0248$), although no differences were apparent for pT3-pT4 tumors (Supplementary figure 6a). Furthermore, in patients with HG NMIBC, higher intratumoral FoxP3$^+$ cell counts were associated with shorter OS and DSS ($P = 0.0115$ and $P = 0.0145$, respectively; Supplementary figure 6b).

FoxP3 and ICOS immunoexpressions were simultaneously evaluated as the latter is a potentially targetable immune checkpoint present on the surface of T cells and particularly

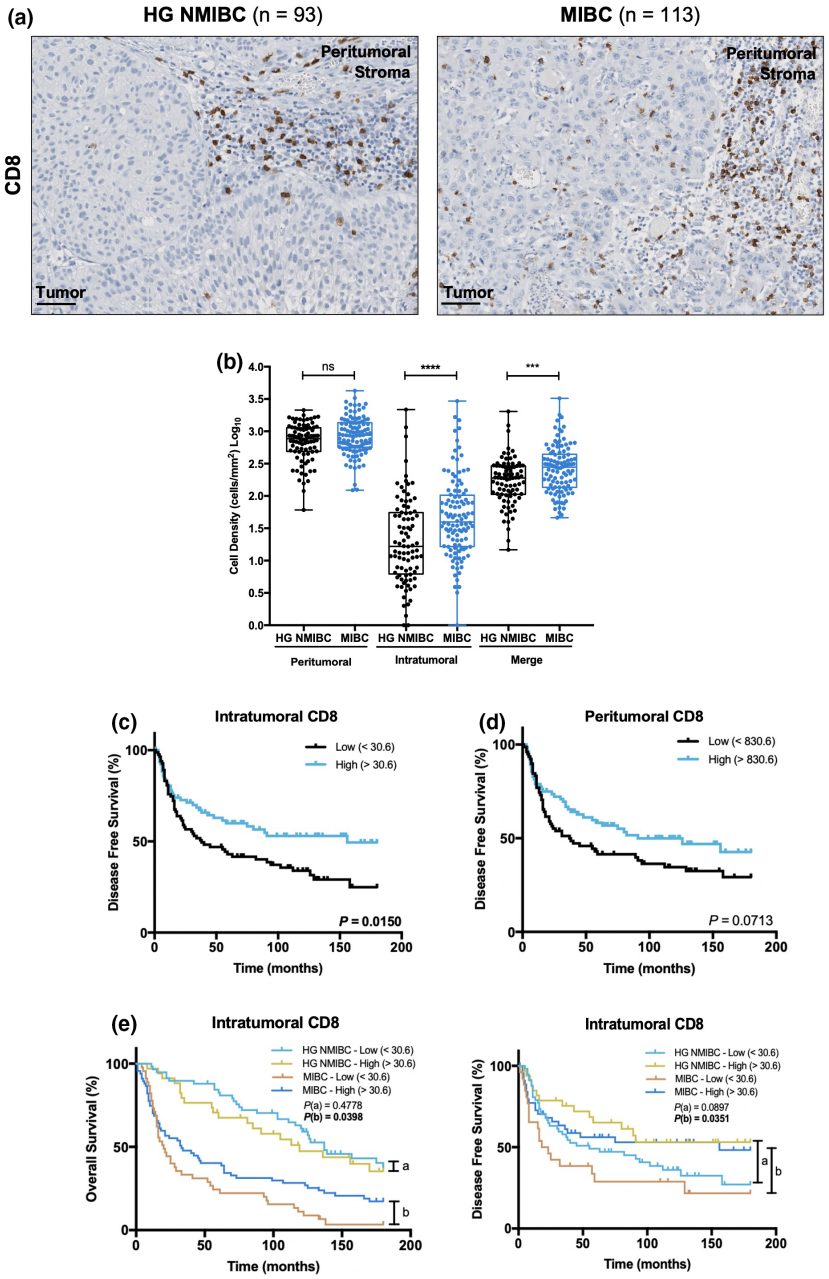

Figure 4. Intratumoral CD8 expression is augmented in MIBC and is associated with improved prognosis. **(a)** Representative examples of CD8 staining in HG NMIBC and MIBC tissue specimens. Notice the increased intratumoral infiltration in MIBC samples. Scale bar = 50 μm. **(b)** Distribution of $CD8^+$ cells density in HG NMIBC ($n = 93$) and MIBC ($n = 113$) samples. The number of positive cells per mm^2 was calculated with QuPath's *Positive Cell Detection* tool. 'Merge' refers to the whole-slide evaluation, considering peritumoral and intratumoral regions together. *P*-values were calculated by the non-parametric Mann–Whitney *U*-test; ns $P > 0.05$, $*P < 0.05$, $**P < 0.01$, $***P < 0.001$, $****P < 0.0001$. Kaplan–Meier estimates of DFS in BlCa patients stratified by peritumoral **(c)** and intratumoral **(d)** CD8 expression. **(e)** Stratified Kaplan–Meier analyses of OS and DFS according to intratumoral CD8 expression and 'HG NMIBC vs MIBC' classification. **(a)** Comparison between 'HG NMIBC Low' and 'HG NMIBC High'; **(b)** Comparison between 'MIBC Low' and 'MIBC High'. Dichotomisation into low and high expression was based on the median value. *P*-values were calculated by the log-rank test. HG NMIBC, high-grade non-muscle invasive bladder cancer; MIBC, muscle-invasive bladder cancer.

overexpressed in T_{regs} (Supplementary figure 7). ICOS positivity was similar in peritumoral stroma of both HG NMIBC and MIBC, but intratumorally increased in MIBC ($P = 0.0142$; Figure 5a). Patients with higher counts of $ICOS^+$ peritumoral cells tended to exhibit longer OS and

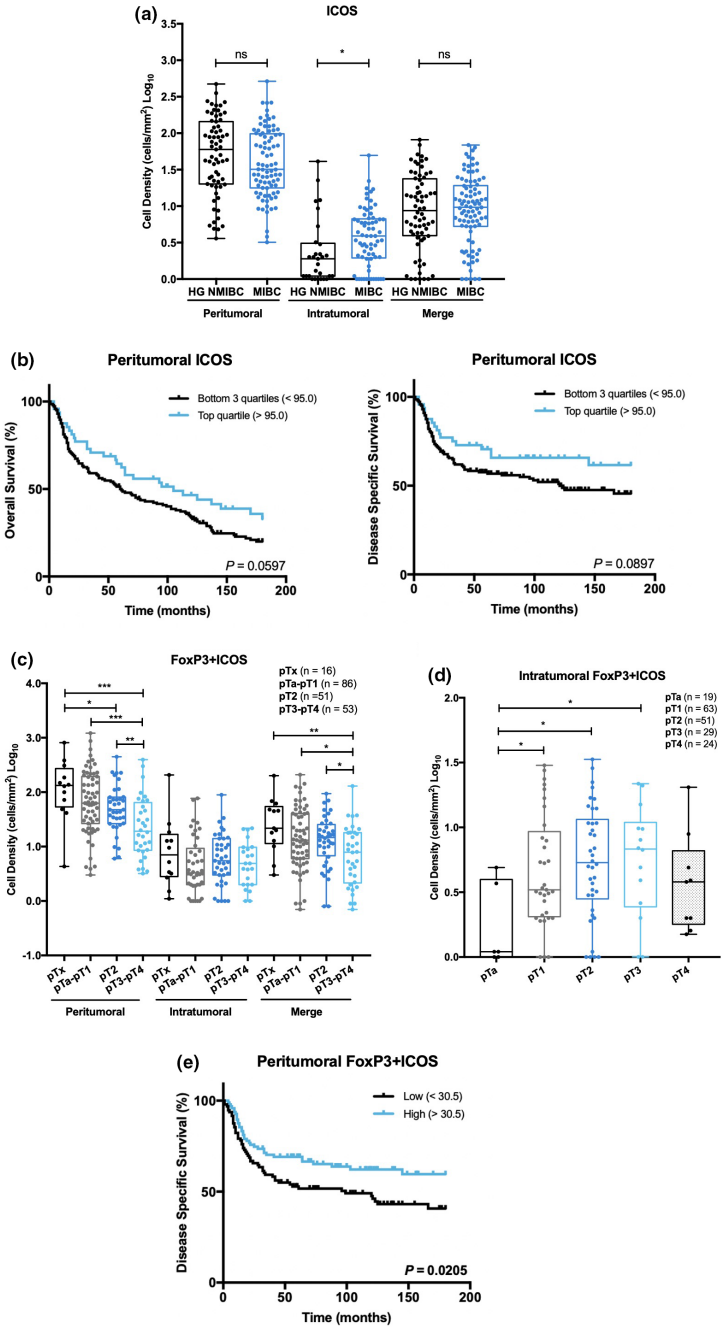

Figure 5. Intratumoral ICOS expression increases in MIBC and tends to associate with prolonged survival. FoxP3^{+}ICOS^{+} cells exhibit different distribution patterns, according to spatial location. **(a)** Distribution of ICOS^{+} cells density in HG NMIBC (n = 93) and MIBC (n = 113) samples. **(b)** Kaplan–Meier estimates of OS and DSS in BlCa patients stratified by peritumoral ICOS single expression. Dichotomisation into low and high expression was based on the percentile 75. **(c)** Distribution of FoxP3^{+}ICOS^{+} cells density in pTx (n = 16), pTa-pT1 (n = 86), pT2 (n = 51) and pT3-pT4 (n = 53) neoplasms. **(d)** Distribution of intratumoral FoxP3^{+}ICOS^{+} cells density across pT stages: pTa (n = 19), pT1 (n = 63), pT2 (n = 51), pT3 (n = 29) and pT4 (n = 24). **(e)** Kaplan–Meier estimates of DSS in BlCa patients stratified by peritumoral FoxP3/ICOS expression. Dichotomisation into low and high expression was based on the median value. *P*-values were calculated by the non-parametric Mann–Whitney *U*-test are depicted in a, c and d; only significant associations ($P < 0.05$) are denoted for simplification purposes in **c** and **d** – $*P < 0.05$, $**P < 0.01$, $***P < 0.001$, $****P < 0.0001$. *P*-values denoted in **b** and **e** were calculated by the log-rank test. 'Merge' refers to the whole-slide evaluation, considering peritumoral and intratumoral regions together. HG NMIBC, high-grade non-muscle invasive bladder cancer; MIBC, muscle-invasive bladder cancer.

DSS, although statistical significance was not achieved ($P = 0.0597$ and $P = 0.0895$, respectively; Figure 5b).

Overall, the absolute number of FoxP3/ICOS double-positive cells was lower than single FoxP3$^+$ cells. In fact, no double-stained cells were observed in 41 cases. Nevertheless, a strong positive correlation was found between the FoxP3$^+$ population and the FoxP3$^+$ICOS$^+$ subset, both peri- and intratumorally ($P < 0.0001$ for both; Spearman's rho = 0.821 and 0.743, respectively). Consistently, a similar distribution pattern was observed for double-stained cells (Figure 5c). Specifically, peritumoral FoxP3$^+$ICOS$^+$ cells density gradually decreased from pTa-pT1 to pT3-pT4 stages ($P = 0.0004$). At the intratumoral level, FoxP3$^+$ICOS$^+$ cells were increased in pT1, pT2 and pT3 stages than in superficial pTa tumors ($P = 0.0416$, $P = 0.0125$ and $P = 0.0264$, respectively), but no significant differences were found between pTa and pT4 (Figure 5d). Importantly, high levels of peritumoral double-positive cells were associated with better DSS ($P = 0.0205$; Figure 5e), whilst no prognostic significance was attributable to tumor-infiltrating FoxP3$^+$ICOS$^+$ cells.

Because anti-PD-L1 therapies are already approved for specific BlCa settings, PD-L1 expression was also evaluated. PD-L1 positivity was generally low and limited to immune cells, with only two samples surpassing the 5% mark. Indeed, 14 cases completely lacked PD-L1 expression. Moreover, no differences were depicted between HG NMIBC and MIBC (Figure 6a and b). Nonetheless, higher PD-L1 expression was significantly associated with shorter DFS ($P = 0.0008$) (Figure 6c). Patients' stratification according to the tumor type ('HG NMIBC vs MIBC') showed that high PD-L1 expression was associated with increased probability of cancer recurrence and cancer-related death in patients with HG NMIBC ($P < 0.0001$, for both) (Figure 6d).

Remarkably, patients with higher PD-L1 positivity depicted significantly increased FoxP3$^+$ICOS$^+$ cells density both in peritumoral and in intratumoral compartments ($P = 0.0004$ and $P = 0.0085$, respectively) (Figure 6e).

Multivariable analyses

Cox-regression models were computed to identify independent factors with influence on OS, DSS and DFS (Supplementary tables 1, 2 and 3, respectively).

Using median values as cut-off, high intratumoral CD68 and merged CD163 levels were found to significantly associate with shorter OS, but this association did not remain significant in a multivariable analysis adjusted for 'HG NMIBC vs MIBC'. Nevertheless, merged ICOS expression was shown to significantly increase OS in the multivariable model (Supplementary table 1).

Regarding DSS, increased counts of CD20$^+$, CD68$^+$ (peritumoral, intratumoral and merge) and CD163$^+$ (merge) cells significantly correlated with poor prognosis. Contrarily, a higher abundance of peritumoral FoxP3$^+$ICOS$^+$ cells disclosed a significant protective effect. However, neither of these associations were retained when adjusting for bladder wall invasion level. As for OS, merged ICOS positively impacted on DSS and the same was observed for high intratumoral CD3 expression (Supplementary table 2).

Finally, augmented levels of intratumoral CD3$^+$ and intratumoral/merged CD8$^+$ cells, as well as PD-L1, independently predicted increased DFS (Supplementary table 3).

DISCUSSION

Systemic immunotherapy has revolutionised cancer treatment and improved patient outcome in multiple malignancies, including BlCa. Nonetheless, and despite associated morbidity, radical cystectomy remains the gold-standard therapeutic option for patients with localised MIBC, as it is a key step towards symptoms relief and long-term survival. Chemotherapy in the neo-adjuvant setting has showed survival benefit, although at the cost of high toxicity. BlCa prognosis has not further improved over the last decades, and neo-adjuvant immunotherapy could open a new avenue in this field,[14] building the path for novel organ-sparing protocols with a more attractive safety profile than chemotherapy. With that in mind, we aimed to characterise and compare the immune infiltrate of HG NMIBC and MIBC, looking for clues that might broaden the spectrum of indications for immunotherapy in BlCa.

In this study, several immune cell populations were addressed through appropriate immunohistochemical markers, selected from the literature. More precisely, CD83 was used for mature DCs,[19] CD20 for B cells,[20] CD68 for TAMs in general,[21] CD163 for M2-like TAMs,[22] CD3 for general T cells,[23] CD8 for cytotoxic T cells, CD4 for

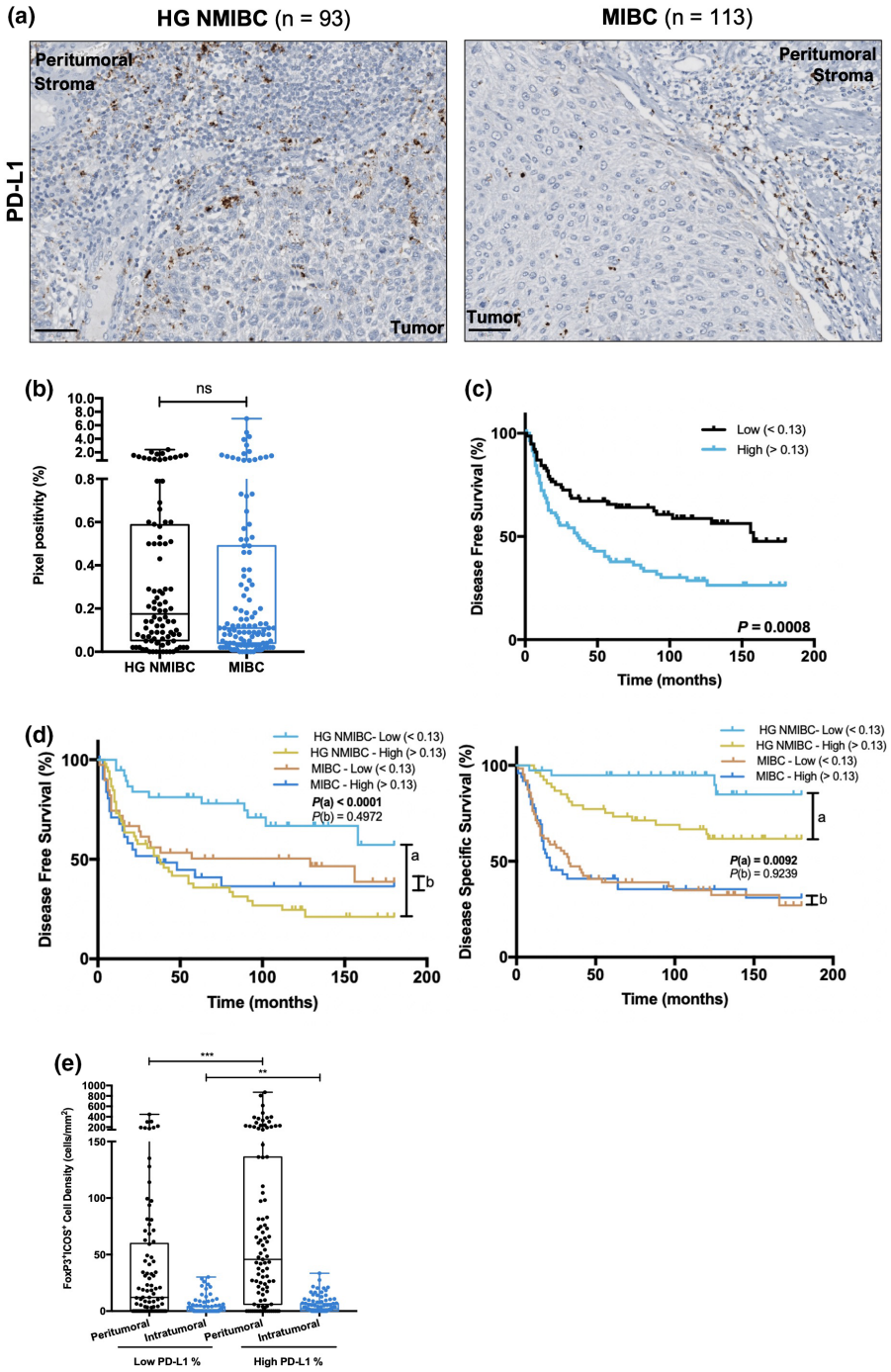

Figure 6. Higher PD-L1 expression negatively impacts disease outcome, especially in HG NMIBC patients, and is associated with increased FoxP3$^+$ICOS$^+$ cell density. **(a)** Representative examples of PD-L1 staining in HG NMIBC and MIBC tissue specimens. Notice the dot–/ant-like staining pattern. Scale bar = 50 μm. **(b)** Distribution of PD-L1 positive percentage in HG NMIBC (n = 93) and MIBC (n = 113) samples. Pixel positivity was assessed with QuPath's *Pixel Classification* tool. **(c)** Kaplan–Meier estimates of DFS in BlCa patients stratified by PD-L1 expression; **(d)** Stratified Kaplan–Meier analyses of DFS and DSS according to PD-L1 expression and 'HG NMIBC vs MIBC' classification. **(a)** Comparison between 'HG NMIBC Low' and 'HG NMIBC High'; **(b)** Comparison between 'MIBC Low' and 'MIBC High'. Dichotomisation into low and high expression was based on the median value. **(e)** Distribution of FoxP3$^+$ICOS$^+$ cells density based on PD-L1-positive percentage. *P*-values calculated by the non-parametric Mann–Whitney *U*-test are depicted in **b** and **e**; only significant associations ($P < 0.05$) are denoted for simplification purposes - $*P < 0.05$, $**P < 0.01$, $***P < 0.001$, $****P < 0.0001$. *P*-values denoted in **c** and **d** were calculated by the log-rank test. HG NMIBC, high-grade non-muscle invasive bladder cancer; MIBC, muscle-invasive bladder cancer.

helper T cells[24] and FoxP3 for T_{regs}.[25] Immune checkpoints were also investigated, namely through PD-L1 and ICOS expression, as they constitute relevant immunotherapeutic targets that may be tackled either individually or in synergy. Identification of a biomarker panel for therapy selection using immunohistochemistry (IHC) is particularly advantageous, as this technique is well-established, readily available and of relatively low cost. Importantly, immunoexpression of each biomarker was quantified using QuPath,[18] which constitutes an important methodological difference from previous works, granting a faster, more precise and reproducible analysis when compared with the traditional manual analysis performed by pathologists, used in other studies focussing on BlCa microenvironment.[26,27] In fact, educated algorithms were applied across all samples, considering each antibody's intensity and staining pattern, which significantly minimised observer-inherent bias. Further validation and implementation of this technique may deeply benefit routine pathological assessment of biomarkers and improve diagnostic quality, contributing for enactment of Precision Medicine. In the present study, spatial distribution of the aforementioned immune markers was also addressed, which is an essential component for assessment of the tumor immune status. A detailed discussion of each immune cell population follows.

Mature DCs, known as efficient antigen-presenting cells, were not generally abundant. This is in line with previous studies that report the predominance of phenotypically immature DCs,[28,29] suggesting a maturity blockage by BlCa cells. In our study, $CD83^+$ DCs were found to be similarly expressed in HG NMIBC and MIBC cases. Furthermore, no prognostic significance was disclosed. Previously, an association between the absence of $CD83^+$ DCs and disease recurrence was reported in NMIBC; however, a high CD83 score seemed to increase the risk of progression to MIBC.[30] Methodological differences, especially concerning the scoring system used, impair a direct comparison with our data. Indeed, those authors considered several tissue structures for CD83 scoring, including distant lymphoid aggregates, which we avoided as these are probably less relevant for antitumor immune response.

B cells are essential drivers of humoral immunity and play an important role in antitumor response,[31] although most studies focus on T cells because of their higher prevalence. In BlCa, controversial data exist concerning this immune cell population and its influence on patients' prognosis. A correlation was found between a higher density of $CD20^+$ B cells within lymphoid aggregates and a prolonged time to recurrence.[27] Similarly, high levels of $CD19^+$ B cells were significantly associated with longer OS in MIBC patients.[32] Albeit CD19 and CD20 are both B-cell lineage-specific, the former's expression starts at the pre-B cell stage, whereas CD20 is expressed somewhat later in B-cell development, being a more specific marker of mature B cells.[33] Thus, comparisons with our data must be made with caution. Interestingly, IL-10 producing regulatory B cells, an immunosuppressive subset, seemed to negatively affect survival.[34] As a very small cohort of MIBC patients ($n = 31$) was used, further validation would be required. Finally, *in vitro* experiments revealed that B cells in the BlCa microenvironment promote metastasis via upregulation of matrix metalloproteinases.[35] In accordance, we found that CD20 was significantly increased in MIBC and associated with a worse DSS. Contrarily to the aforementioned studies, peritumoral B cells, but not lymphoid aggregates, were included in the analysis. Thus, we are tempted to speculate whether the spatial location of B lymphocytes determines their functionality and, thus, detailed functional characterisation is required to accurately decipher the behaviour of this population and the consequent impact on BlCa outcome. Remarkably, CD20 was also found to be differentially expressed between genders, showing increased levels in men. Nevertheless, it should be noted that just 44 women are being compared with 162 men and, thus, the reach of this observation may be limited. Distinct genomic subtypes with gender-related molecular disparities have been described in NMIBC,[36] and additional efforts to understand the factors underlying gender bias might help improve quality of care of BlCa patients.

TAMs are the most frequent innate immune cells in the tumor microenvironment, known for their phenotypic plasticity and role as antigen-presenting cells. In tumors, TAMs are usually polarised towards an immunosuppressive M2 phenotype, promoting tumor growth and metastasis.[37] The tumorigenic role of TAMs has been widely described in BlCa. Already in 2000, TAMs ($CD68^+$) counts were found to be

significantly higher in MIBC and associated with distant metastasis, vascular invasion, and decreased 5-year survival rate.[38] Subsequently, other immunohistochemical analyses correlated $CD68^+$ TAMs with worse DSS in MIBC[39] and with recurrence in NMIBC.[30] Our findings are consistent with previous studies, as $CD68^+$ and $CD163^+$ cells were increased in MIBC, both in the peritumoral stroma and within the tumor, negatively correlating with survival. Thus, TAMs (mainly M2 polarised) seem to contribute to tumor growth and consequent deep invasion of the bladder wall, acting on the invasive margin and in direct contact with tumor cells. Furthermore, our work highlights that TAMs may be used to identify patients who might benefit from intravesical mitomycin, as previously suggested regarding intravesical Bacillus Calmette-Guérin[40] and adjuvant chemotherapy.[41]

T lymphocytes are a major focus of immuno-oncology research, because of their central role in antitumor immunity and association with clinical outcomes. T cells are highly heterogeneous, and a particular immune response reflects a fine balance between distinct subpopulations. Hence, we first characterised this population using a general T-cell marker (CD3) and then addressed two broad classes: $CD8^+$ cytotoxic and $CD4^+$ helper T cells. Cytotoxic T cells are the main effectors of the immune system and were found to be predominant in the overall T-cell population.[42] Accordingly, we found that CD3 and CD8 expression exhibited an identical distribution pattern and prognostic significance. Both markers were similarly expressed in the peritumoral stroma of HG NMIBC and MIBC; nonetheless, significantly higher expression within the tumor was observed in MIBC.[39] Furthermore, increased counts of intratumoral $CD3^+$ and $CD8^+$ cells independently and positively impacted DFS. This observation is in line with prior studies conducted on several cancer types, including BlCa,[43,44] supporting the hypothesis that infiltrating T cells have a protective effect, especially the $CD8^+$ subset, because of their ability to induce tumor cell apoptosis through cytolytic mediators, such as perforin and granzyme. Remarkably, the spatial location of $CD8^+$ T cells within the tissue was found relevant as tumor infiltration *per se* was associated with a favorable outcome.[27]

Helper T cells ($CD4^+$) simultaneously integrate different stimuli from the environment and consequently acquire a multitude of functional phenotypes, either with tumoricidal or with tumorigenic activity.[42] In our study, $CD4^+$ T cells were found in most tumors, but in lower frequency than the cytotoxic class. Curiously, CD4 expression was higher in the peritumoral stroma of HG NMIBC, but augmented in the intratumoral compartment of MIBC, demonstrating a more efficient infiltration in the latter group. High $CD4^+$ T-cell density was previously found to correlate with poor prognosis in NMIBC.[45] Likewise, a gene expression-based study found a correlation between a high CD3/CD4 ratio and better survival in MIBC.[46] These observations may reflect the predominance of immunosuppressive $CD4^+$ subsets, although the aforementioned studies lack deeper functional phenotyping. Recently, cytotoxic $CD4^+$ T cell states directly involved in tumor cell killing were identified in MIBC,[47] highlighting the importance of more precise identification of T-cell subtypes within the tumor microenvironment for a better understanding of tumor immunity, and its clinical manipulation.

In this study, we further characterised $CD4^+$ T cells focussing on T_{regs}, well-known for their tumor-promoting activity in various cancer types.[48] However, the role of this immune cell population in BlCa remains unclear, considering the contradictory findings reported. Various studies associated increased infiltration of $FoxP3^+$ T cells with poor prognosis, both in NMIBC and in MIBC.[49–51] Contrarily, other studies correlated $FoxP3^+$ lymphocytes with improved OS[52] and time to recurrence.[27] $FoxP3^+$ T_{regs} located at the invasive margin seemed to have a positive impact, through inhibition of MMP2, a key factor for tumor invasion.[53] These findings demonstrated that the prognostic value may depend on the relative spatial location of T_{regs} within the tumor. Our results further sustain this hypothesis, as peritumoral $FoxP3^+$ cells were decreased at advanced disease stages, although not correlated with prognosis, whereas their intratumoral counterparts disclosed the reverse distribution pattern and negatively impacted on prognosis, particularly in NMIBC. T_{regs} may exhibit multiple phenotypes with defined functional activity,[54,55] and, thus, it is also possible that a FoxP3-based characterisation is too simplistic and additional markers are needed to fully phenotype T_{regs} and understand their prognostic significance in BlCa. In this regard, it is also important to highlight that FoxP3 was found expressed in the absence of

CD4 in a few samples, indicating the presence of a FoxP3-expressing subset other than T_{regs}. Previous studies have reported a temporary expression of this transcriptional regulator during the activation process of $CD4^+$ and $CD8^+$ effector T cells, which is insufficient to induce an immunosuppressive phenotype, characterised by the ability to limit proinflammatory factors, such as interferon-γ.[56,57] This is consistent with the lymphoid morphology of the observed FoxP3 stained cells and further sustains the hypothesis that additional markers are needed for accurate T_{regs} characterisation.

Thus, we also investigated the role of ICOS, as evidence suggests its highest expression on the surface of T_{regs},[58] being pivotal for their homeostasis, survival and suppressive activity. Indeed, $ICOS^{high}$ T_{regs} correlated with an increased production of the anti-inflammatory cytokine IL-10, making them particularly immunosuppressive.[59] Hence, ICOS constitutes a relevant immunotherapeutic target for T_{regs} depletion, as a strategy to enhance antitumor immunity. Regarding ICOS assessment, intratumoral single-positive cells were increased in MIBC, but no differences were observed at the peritumoral level, than in HG NMIBC. Therefore, ICOS and CD8 shared an identical distribution pattern, which allows us to conclude that most ICOS single-positive cells are, indeed, $CD8^+$ effector T cells. ICOS interaction with its ligand, ICOS-L, constitutes a costimulatory signal that induces the production of a wide range of cytokines, either pro- or anti-inflammatory.[17] Likewise, $CD8^+ICOS^+$ T cells exhibit enhanced proliferation and antitumor response, which might justify the longer survival trend observed in patients with increased ICOS single-positive cells. When looking into $FoxP3^+ICOS^+$ T cells, a differential behaviour according to the spatial location was observed, favoring, once more, the hypothesis that T_{regs} role in BlCa likely depends on its spatial location within the tumor landscape. Indeed, peritumoral T_{regs} positive for ICOS gradually decreased in advanced pT stages and were found to positively impact on DSS. Contrarily, in the intratumoral region, this subpopulation tended to increase in density, and no significant impact was disclosed on patient survival.

PD-L1 expression was also investigated and correlated with ICOS to address whether a combinatorial therapeutic approach would eventually benefit BlCa patients. PD-L1 is a well-known immune checkpoint molecule involved in T-cell exhaustion, and its expression has been widely correlated with poor prognosis in several human cancers, including BlCa.[60–62] However, inconsistent results have been recently reported, suggesting a positive impact of PD-L1 on survival, particularly if expressed by immune cells.[27,63] In our cohort, PD-L1 positivity was generally low and even absent in some cases; furthermore, no differences were observed between HG NMIBC and MIBC, which is in accordance with a previous study.[63] Interestingly, high PD-L1 expression was significantly associated with shorter DFS, including in a multivariable model adjusted for the degree of bladder wall invasion ('HG NMIBC vs MIBC'). Of note, PD-L1 pixel positivity was quantified according to the SP142 scoring algorithm for urothelial carcinoma, which reflects the proportion of tumor area (including stroma) covered by positive immune cells.[64] SP142 is known to detect fewer urothelial tumor cells than other clones[65,66] and, accordingly, practically all the staining in our samples matched immune cells. A median value cut-off was considered as there was an extremely low representativity of patients with a PD-L1 expression level $\geq$ 5%. Conflicting data on PD-L1 prognostic value may be explained by differences in anti-PD-L1 antibodies, scoring algorithms, prognostic cut-off values and preanalytical variables. Standardised criteria for the evaluation of PD-L1 positivity are needed if an accurate interpretation of its prognostic value is desired.

Remarkably, we found that patients with higher PD-L1 expression exhibited higher levels of $ICOS^+$ T_{regs}, both peri- and intratumorally. As the same patients were reported to have and increased likelihood of disease recurrence, a complementary therapeutic strategy involving T_{regs} abrogation might be of benefit. Nonetheless, this topic requires further explorations, preferably in a more heterogeneous cohort that includes patients with higher PD-L1 positivity, which would be eligible for treatment with Atezolizumab (assessed by the SP142 assay). Also, an in-depth understanding of how this ICI affects the BlCa microenvironment, particularly $FoxP3^+ICOS^+$ T_{regs}, may provide valuable information about a potential combinatorial therapy.

Our findings, in line with the few already published studies, support the clinical relevance of immune markers in BlCa prognostication. BlCa is a well-known inflamed tumor, densely populated by distinct immune cells, and, to the best of our

knowledge, we are the first to provide such a detailed insight into BlCa immune microenvironment. Significant differences were detected between the immunoprofile of HG NMIBC and MIBC that may be used for the selection of a biomarker panel with potential to identify patients suitable for treatment with immunotherapy, and appropriate targets. For instance, MIBC was undoubtedly enriched in TAMs, B cells and $CD8^+$ T cells and, thus, therapeutic strategies that inhibit or enhance these populations (as appropriate) are potentially beneficial for patients with invasive disease. In turn, PD-L1 immunoexpression was identical in both types of tumors, suggesting that anti-PD-L1 ICIs might be considered in localised MIBC, eventually in combination with other immunotherapeutic agents, in an attempt to increase the still minority of BlCa patients (about 20%) which benefit from these immunotherapies.[67–69]

Limitations of our work include its retrospective design, as well as the known limitations of IHC, although the computerised quantification of staining significantly decreased the inherent subjectivity. It should be noted that the small number of patients within groups may also be limiting, having a negative impact on the multivariable analyses results. Moreover, molecular classification of BlCa, which is known to influence immune infiltration,[70–72] was not addressed in this study. Efforts are being made, including by our group,[73] to translate BlCa molecular subtypes acknowledged by transcriptomic analyses to routine practice using IHC evaluation. Investigating additional predictive biomarkers of response to immunotherapy would be advantageous, as a strategy to improve predictive power. Tumor mutational burden and microsatellite instability status are promising candidates, as suggested in the literature.[74,75]

CONCLUSION

Immunoprofiling of HG NMIBC and MIBC unravelled important differences, but also relevant similarities, between the immune infiltrate composition of both BlCa types. Our results suggest that immunotherapy may be beneficial in the management of patients with localised MIBC, although the most appropriate target molecules/immune cell populations may differ from those tackled in HG NMIBC. Emphasis on TAMs, B cells and $CD8^+$ cytotoxic T cells seems reasonable considering they are particularly abundant in MIBC. Furthermore, we also identified ICOS as a potential immunotherapeutic target in BlCa (although further validation is needed) which, through T_{regs} depletion, may increase the efficacy of existing immunotherapies.

METHODS

Patients and samples

The study cohort included 206 patients diagnosed with urothelial carcinoma of the bladder (HG NMIBC or MIBC) between 1996 and 2007 at the Portuguese Oncology Institute of Porto (IPO Porto), Portugal. For each case, the most representative block (higher ratio of tumor cells, less necrosis and enough tissue for the study) of therapy-naïve, formalin-fixed paraffin-embedded tissue specimen obtained either from transurethral resection or from cystectomy was selected from the archives of the Department of Pathology by a dedicated uropathologist. Histological classification and tumor staging were re-coded in accordance with the 2016 World Health Organisation Classification of Tumors of the Urinary System and Male Genital Organs[4] and the 8th edition of the American Joint Committee on Cancer staging manual, respectively.[76] From the selected samples, 4 μm-thick consecutive sections were performed for IHC assays. Relevant clinical data were retrieved from clinical files. All samples derived from routinely archived material (formalin-fixed paraffin-embedded tissues of surgical specimens) which were used after anonymisation. Thus, consent to use the samples was waived according to Portuguese Law, through approval by the Institutional Review Board (Comissão de Ética para a Saúde) of IPO Porto (CES-IPOP-06R1/019).

Immunohistochemistry

Expression of a set of immune biomarkers in BlCa tissues was assessed by IHC, comprising CD83, CD20, CD68, CD163, CD3, CD8, CD4, FoxP3, ICOS and PD-L1. Details on antibodies used, respective clones, dilutions, positive controls and vendors are depicted in Supplementary table 1. First, all tissue sections were deparaffinised in xylene (Sigma Aldrich, Steinheim, Germany) and rehydrated in a graded alcohol series. Then, antigens were retrieved with previously standardised conditions (Supplementary table 1). For CD8, CD4, ICOS and PD-L1, each chromogen reaction was fully automated, using BenchMark ULTRA Slide Staining System (Roche, Basel, Switzerland). An appropriate positive control was included in each slide. The remaining markers were manually stained using a routine protocol which was adapted for the usage of reagents from the *ultra*View Universal Diaminobenzidine (DAB) Detection Kit (Roche). Briefly, after antigen retrieval, tissue sections were delimited with a hydrophobic pen (Dako, Glostrup, Denmark) and incubated for 5 min with *ultra*View Universal DAB Inhibitor (Roche), a 3% H_2O_2 solution, to block endogenous peroxidase activity, followed by a 5-min incubation with Protein Block (Leica Biosystems, Wetzlar, Germany) to

reduce non-specific background staining. Subsequently, primary antibodies were incubated for 1 h, at room temperature, as appropriate (Supplementary table 1). One positive control was included in each IHC run. Thereafter, slides were incubated with *ultra*View Universal HRP Multimer (Roche), a cocktail of enzyme-labelled secondary antibodies, for 10 min. Washes between steps were performed with Tris-buffered saline-Tween 20 1×. DAB (Sigma Aldrich), diluted in 1× phosphate-buffered saline, was the chromogen used and tissues were counterstained with haematoxylin (Leica Biosystems) for 1 min. Finally, samples were dehydrated, diaphanised and mounted with Entellan (Merck-Millipore, Darmstadt, Germany).

Evaluation of immunohistochemical staining – digital image analysis

QuPath software

QuPath (https://qupath.github.io) is an open-source, user-friendly software for digital pathology and whole-slide imaging analysis.[18] Briefly, the software was written using Java 8 and includes a graphic interface for annotation and whole-slide visualisation. Moreover, a wide range of novel built-in algorithms is available, and interactive machine learning tools, such as object and pixel classification, allowing for workflow customisation. Image analyses in this study were performed using QuPath version 0.2.3 on a Macbook Pro (2,9 GHz, Intel Core i5, 8 GB RAM).

Immune biomarkers spatial analysis

Following IHC staining, all slides were scanned in a Ventana DP200 slide scanner (Roche) at ×20 magnification. Whole-slide images were imported to QuPath's application, and separate projects were created for each immune biomarker. Ten regions of interest per slide were defined, five in the peritumoral stroma contiguous to the tumor and five inside the area occupied by viable tumor cells. Peritumoral and intratumoral protein quantification was performed either individually or in combination ('merge' = the sum of peritumoral and intratumoral positivity divided by the total area of the 10 selected regions of interest).

Three distinct image analysis protocols were optimised, according to staining-intrinsic characteristics. More precisely, CD83, CD20, CD3, CD8 and CD4 were single-stained with DAB and exhibited a clear membrane staining. Thus, positive cells were evaluated using the following path: *Analyse* → *Cell Detection* → *Positive Cell Detection*. A threshold was manually refined, in accordance with the staining intensity of each antibody and immune cells dimension. All regions of interest were analysed and the number of positive cells per mm^2 was calculated, based on the absolute number of positive cells and area detected.

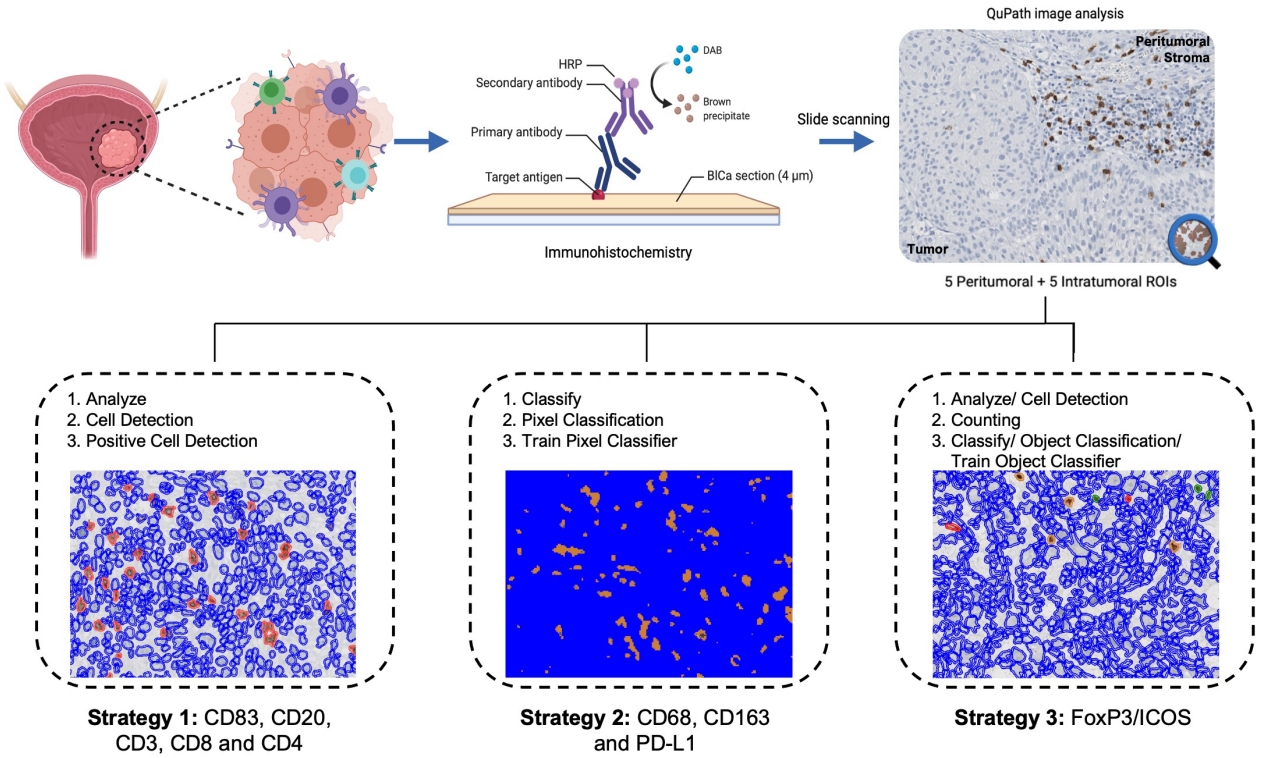

Figure 7. Schematic representation of experimental methodology and image analysis workflow. IHC staining of HG NMIBC and MIBC samples and subsequent whole-slide image analysis with QuPath. BlCa, bladder cancer; DAB, Diaminobenzidine; HRP, horseradish peroxidase; ROIs, regions of interest.

Conversely, CD68, CD163 and PD-L1 displayed a diffuse and scattered staining pattern. Hence, pixel positivity was evaluated instead, reflecting the area covered by DAB's brown staining within defined regions of interest. For this type of analysis, an interactive machine learning tool (*Classify → Pixel Classification → Train Pixel Classifier*) allowed classifier training using representative areas, positive/negative for staining. PD-L1 immunoexpression was scored according to the established Ventana's SP142 scoring algorithm for urothelial carcinoma.[64]

Finally, FoxP3 and ICOS were double-stained using DAB and Fast Red/Naphthol chromogens, respectively. Consequently, there was a need to distinguish single FoxP3-positive, single-ICOS-positive, double-positive, and negative cells. Initially, cells within regions of interest were automatically detected with appropriate criteria (*Analyse → Cell Detection → Cell Detection*). Then, the *Counting* tool was used to manually select and classify cells belonging to each of the four mentioned groups. Again, an interactive machine learning approach (*Classify → Object Classification → Train Object Classifier*) was applied to train the classifier, gradually improving its sensitivity. The final measurement was the number of positive cells of each class per area (mm^2).

Once the threshold was defined, regardless of the path, it was consistently applied across all samples. Importantly, positive cells detection (both in single and in double staining) was manually confirmed in all images, and corrections were made, if necessary.

A summary of IHC quantification strategies is illustrated in Figure 7.

Statistical analyses

Statistical analyses were performed using IBM SPSS Statistics version 28.0 for Macintosh (Armonk, NY, USA) and GraphPad Prism 7.3 (GraphPad Software, La Jolla, California, USA). The non-parametric Mann–Whitney *U*-test was used to compare distributions of immunological markers' expression (continuous variables) between pairs of groups. Investigation of interrelationships between continuous variables was performed with Spearman's non-parametric correlation test. For survival analyses, expression data were dichotomised into 'low' and 'high' categories, using median or percentile 75 (ICOS immunoexpression) values as the cut-off. Kaplan–Meier survival curves were generated, and the log-rank test (comparison of pairs of curves, as appropriate) was applied to assess differences in OS, DSS and DFS according to each marker's expression, either individually or in combination with the 'HG NMIBC vs MIBC' classification of samples. OS was defined as the time from diagnosis to death or last follow-up; DSS as time from diagnosis to cancer-related death or last follow-up/death from other causes, and DFS as time from diagnosis to the date of disease recurrence (biopsy or imaging confirmation) or death/last follow-up. Cox-regression analyses were used to evaluate the impact of the studied biomarkers on OS, DSS and DFS, through estimation of the respective hazard ratio with 95% confidence intervals. Multivariable analysis was also computed, adjusted for 'HG NMIBC vs MIBC' status. *P*-values < 0.05 were considered statistically significant for all tests.

ACKNOWLEDGMENTS

This study was funded by the Research Center of Portuguese Institute of Porto (CI-IPOP-27-2016) and partially by Kymab Ltd, a Sanofi Company. JL is a recipient of a FCT – Fundação para a Ciência e Tecnologia fellowship (SFRH/BD/132751/2017). CML was supported by a fellowship from University of Campania 'Luigi Vanvitelli', 80138 Naples, Italy. BCTF contract is funded by CI-IPOP/PD/Kymab.

AUTHOR CONTRIBUTIONS

Nicole Viveiros: Data curation; formal analysis; methodology; writing – original draft. **Bianca CT Flores:** Supervision. **João Lobo:** Data curation; formal analysis. **Cláudia Martins-Lima:** Methodology. **Mariana Cantante:** Methodology. **Paula Lopes:** Methodology. **Cecilia Deantonio:** Writing – review and editing. **Cintia Palu:** Writing – review and editing. **Richard CA Sainson:** Writing – review and editing. **Rui Henrique:** Supervision; writing – review and editing. **Carmen Jerónimo:** Supervision; writing – review and editing.

CONFLICT OF INTEREST

CD and CP are employees of Kymab Ltd, a Sanofi Company. All the remaining authors declare that they have no competing interests.

ETHICS APPROVAL

This study was approved by the Ethics Committee (CES-IPO-06R1/019) of Portuguese Oncology Institute of Porto, Portugal. All procedures performed in tasks involving human participants were in accordance with the ethical standards of the institutional and/or national research committee and with the 1964 Helsinki declaration and its later amendments or comparable ethical standards.

DATA AVAILABILITY STATEMENT

All data generated or analysed during this study are included in this published article and its Supplementary Information files.

REFERENCES

1. Sung H, Ferlay J, Siegel RL *et al*. Global cancer statistics 2020: GLOBOCAN estimates of incidence and mortality worldwide for 36 cancers in 185 countries. *CA Cancer J Clin* 2021; **71**: 209–249.
2. Botteman MF, Pashos CL, Redaelli A, Laskin B, Hauser R. The health economics of bladder cancer. *Pharmacoeconomics* 2003; **21**: 1315–1330.
3. Messing EM. Financial toxicity of having bladder cancer. *Bladder Cancer* 2018; **4**: 351–352.
4. Moch H, Cubilla AL, Humphrey PA, Reuter VE, Ulbright TM. *The 2016 WHO Classification of Tumors of the Urinary System and Male Genital Organs*. 4th ed. IARC: Lyon; 2016.

5. Richters A, Aben KKH, Kiemeney LALM. The global burden of urinary bladder cancer: an update. *World J Urol* 2020; **38**: 1895–1904.
6. Pardoll DM. The blockade of immune checkpoints in cancer immunotherapy. *Nat Rev Cancer* 2012; **12**: 252–264.
7. Upadhaya S, Hubbard-Lucey VM, Yu JX. Immuno-oncology drug development forges on despite COVID-19. *Nat Rev Drug Discov* 2020; **19**: 751–752.
8. Morales A, Eidinger D, Bruce AW. Intracavitary bacillus Calmette-guerin in the treatment of superficial bladder tumors. *J Urol* 1976; **116**: 180–182.
9. Osterman C, Milowsky M. New and emerging therapies in the Management of Bladder Cancer. *F1000Res* 2020; **9**: 1146.
10. Griffiths G, Hall R, Sylvester R, Raghavan D, Parmar MK. International phase III trial assessing neoadjuvant cisplatin, methotrexate, and vinblastine chemotherapy for muscle-invasive bladder cancer: long-term results of the BA06 30894 trial. *J Clin Oncol* 2011; **29**: 2171–2177.
11. Yin M, Joshi M, Meijer RP *et al*. Neoadjuvant chemotherapy for muscle-invasive bladder cancer: a systematic review and two-step meta-analysis. *Oncologist* 2016; **21**: 708–715.
12. Salminen AP, Montoya Perez I, Klén R *et al*. Adverse events during neoadjuvant chemotherapy for muscle invasive bladder cancer. *Bladder Cancer* 2019; **5**: 273–279.
13. Pederzoli F, Bandini M, Marandino L *et al*. Neoadjuvant chemotherapy or immunotherapy for clinical T2N0 muscle-invasive bladder cancer: time to change the paradigm? *Eur Urol Oncol* 2021; **4**: 1006–1010.
14. Mancini M, Righetto M, Noessner E. Checkpoint inhibition in bladder cancer: clinical expectations, current evidence, and proposal of future strategies based on a tumor-specific immunobiological approach. *Cancer* 2021; **13**: 6016.
15. Hutloff A, Dittrich AM, Beier KC *et al*. ICOS is an inducible T-cell co-stimulator structurally and functionally related to CD28. *Nature* 1999; **397**: 263–266.
16. Rudd CE, Schneider H. Unifying concepts in CD28, ICOS and CTLA4 co-receptor signalling. *Nat Rev Immunol* 2003; **3**: 544–556.
17. Solinas C, Gu-Trantien C, Willard-Gallo K. The rationale behind targeting the ICOS-ICOS ligand costimulatory pathway in cancer immunotherapy. *ESMO Open* 2020; **5**: e000544.
18. Bankhead P, Loughrey MB, Fernández JA *et al*. QuPath: open source software for digital pathology image analysis. *Sci Rep* 2017; **7**: 16878–16883.
19. Prechtel AT, Steinkasserer A. CD83: an update on functions and prospects of the maturation marker of dendritic cells. *Arch Dermatol Res* 2007; **299**: 59–69.
20. Adams H, Liebisch P, Schmid P, Dirnhofer S, Tzankov A. Diagnostic utility of the B-cell lineage markers CD20, CD79a, PAX5, and CD19 in paraffin-embedded tissues from lymphoid neoplasms. *Appl Immunohistochem Mol Morphol* 2009; **17**: 96–101.
21. Holness C, Simmons D. Molecular cloning of CD68, a human macrophage marker related to lysosomal glycoproteins. *Blood* 1993; **81**: 1607–1613.
22. Ambarus CA, Krausz S, van Eijk M *et al*. Systematic validation of specific phenotypic markers for *in vitro* polarized human macrophages. *J Immunol Methods* 2012; **375**: 196–206.
23. Furley AJ, Mizutani S, Weilbaecher K *et al*. Developmentally regulated rearrangement and expression of genes encoding the T cell receptor-T3 complex. *Cell* 1986; **46**: 75–87.
24. Appay V, van Lier RAW, Sallusto F, Roederer M. Phenotype and function of human T lymphocyte subsets: consensus and issues. *Cytometry A* 2008; **73A**: 975–983.
25. Fontenot JD, Gavin MA, Rudensky AY. Foxp3 programs the development and function of $CD4^+$ $CD25^+$ regulatory T cells. *Nat Immunol* 2003; **4**: 330–336.
26. Li H, Zhang Q, Shuman L *et al*. Evaluation of PD-L1 and other immune markers in bladder urothelial carcinoma stratified by histologic variants and molecular subtypes. *Sci Rep* 2020; **10**: 1439.
27. Wahlin S, Nodin B, Leandersson K, Boman K, Jirström K. Clinical impact of T cells, B cells and the PD-1/PD-L1 pathway in muscle invasive bladder cancer: a comparative study of transurethral resection and cystectomy specimens. *Onco Targets Ther* 2019; **8**: e1644108.
28. Troy AJ, Davidson PJT, Atkinson CH, Hart DNJ. CD1A dendritic cells predominate in transitional cell carcinoma of bladder and kidney but are minimally activated. *J Urol* 1999; **161**: 1962–1967.
29. Beatty JD, Islam S, North ME, Knight SC, Ogden CW. Urine dendritic cells: a noninvasive probe for immune activity in bladder cancer? *BJU Int* 2004; **94**: 1377–1383.
30. Ayari C, LaRue H, Hovington H *et al*. High level of mature tumor-infiltrating dendritic cells predicts progression to muscle invasion in bladder cancer. *Hum Pathol* 2013; **44**: 1630–1637.
31. Guo FF, Cui JW. The role of tumor-infiltrating B cells in tumor immunity. *J Oncol* 2019: e2592419.
32. Jiang Q, Fu Q, Chang Y *et al*. $CD19^+$ tumor-infiltrating B-cells prime $CD4^+$ T-cell immunity and predict platinum-based chemotherapy efficacy in muscle-invasive bladder cancer. *Cancer Immunol Immunother* 2019; **68**: 45–56.
33. Forsthuber TG, Cimbora DM, Ratchford JN, Katz E, Stüve O. B cell-based therapies in CNS autoimmunity: differentiating CD19 and CD20 as therapeutic targets. *Ther Adv Neurol Disord* 2018; **11**: e1756286418761697.
34. Zirakzadeh AA, Sherif A, Rosenblatt R *et al*. Tumor-associated B cells in urothelial urinary bladder cancer. *Scand J Immunol* 2020; **91**: e12830.
35. Ou Z, Wang Y, Liu L *et al*. Tumor microenvironment B cells increase bladder cancer metastasis via modulation of the IL-8/androgen receptor (AR)/MMPs signals. *Oncotarget* 2015; **6**: 26065–26078.
36. Hurst CD, Alder O, Platt FM *et al*. Genomic subtypes of non-invasive bladder cancer with distinct metabolic profile and female gender bias in KDM6A mutation frequency. *Cancer Cell* 2017; **32**: 701–715.e707.
37. Yang Q, Guo N, Zhou Y, Chen J, Wei Q, Han M. The role of tumor-associated macrophages (TAMs) in tumor progression and relevant advance in targeted therapy. *Acta Pharm Sin B* 2020; **10**: 2156–2170.

38. Hanada T, Nakagawa M, Emoto A, Nomura T, Nasu N, Nomura Y. Prognostic value of tumor-associated macrophage count in human bladder cancer. *Int J Urol* 2000; **7**: 263–269.
39. Sjödahl G, Lövgren K, Lauss M *et al*. Infiltration of $CD3^+$ and $CD68^+$ cells in bladder cancer is subtype specific and affects the outcome of patients with muscle-invasive tumors. *Urol Oncol* 2014; **32**: 791–797.
40. Lima L, Oliveira D, Tavares A *et al*. The predominance of M2-polarized macrophages in the stroma of low-hypoxic bladder tumors is associated with BCG immunotherapy failure. *Urol Oncol* 2014; **32**: 449–457.
41. Qi Y, Chang Y, Wang Z *et al*. Tumor-associated macrophages expressing galectin-9 identify immunoevasive subtype muscle-invasive bladder cancer with poor prognosis but favorable adjuvant chemotherapeutic response. *Cancer Immunol Immunother* 2019; **68**: 2067–2080.
42. Waldman AD, Fritz JM, Lenardo MJ. A guide to cancer immunotherapy: from T cell basic science to clinical practice. *Nat Rev Immunol* 2020; **20**: 651–668.
43. Sharma P, Shen Y, Wen S *et al*. CD8 tumor-infiltrating lymphocytes are predictive of survival in muscle-invasive urothelial carcinoma. *Proc Natl Acad Sci USA* 2007; **104**: 3967–3972.
44. Faraj SF, Munari E, Guner G *et al*. Assessment of tumoral PD-L1 expression and intratumoral $CD8^+$ T cells in urothelial carcinoma. *Urology* 2015; **85**: e1–e6.
45. Chiba T, Ohtani H, Mizoi T *et al*. Intraepithelial $CD8^+$ T-cell-count becomes a prognostic factor after a longer follow-up period in human colorectal carcinoma: possible association with suppression of micrometastasis. *Br J Cancer* 2004; **91**: 1711–1717.
46. Shi M, Meng X, Wu Q, Zhou X. High CD3D/CD4 ratio predicts better survival in muscle-invasive bladder cancer. *Cancer Manag Res* 2019; **11**: 2987–2995.
47. Oh DY, Kwek SS, Raju SS *et al*. Intratumoral $CD4^+$ T cells mediate anti-tumor cytotoxicity in human bladder cancer. *Cell* 2020; **181**: 1612–1625.
48. Togashi Y, Shitara K, Nishikawa H. Regulatory T cells in cancer immunosuppression - implications for anticancer therapy. *Nat Rev Clin Oncol* 2019; **16**: 356–371.
49. Murai R, Itoh Y, Kageyama S *et al*. Prediction of intravesical recurrence of non-muscle-invasive bladder cancer by evaluation of intratumoral $Foxp3^+$ T cells in the primary transurethral resection of bladder tumor specimens. *PLoS One* 2018; **13**: e0204745.
50. Miyake M, Tatsumi Y, Gotoh D *et al*. Regulatory T cells and tumor-associated macrophages in the tumor microenvironment in non-muscle invasive bladder cancer treated with intravesical Bacille Calmette-Guérin: a long-term follow-up study of a Japanese cohort. *Int J Mol Sci* 2017; **18**: 2186–2195.
51. Horn T, Laus J, Seitz AK *et al*. The prognostic effect of tumor-infiltrating lymphocytic subpopulations in bladder cancer. *World J Urol* 2016; **34**: 181–187.
52. Winerdal ME, Marits P, Winerdal M *et al*. FOXP3 and survival in urinary bladder cancer. *BJU Int* 2011; **108**: 1672–1678.
53. Winerdal ME, Krantz D, Hartana CA *et al*. Urinary bladder cancer Tregs suppress MMP2 and potentially regulate invasiveness. *Cancer Immunol Res* 2018; **6**: 528–538.
54. Dees S, Ganesan R, Singh S, Grewal IS. Regulatory T cell targeting in cancer: emerging strategies in immunotherapy. *Eur J Immunol* 2021; **51**: 280–291.
55. Li C, Jiang P, Wei S, Xu X, Wang J. Regulatory T cells in tumor microenvironment: new mechanisms, potential therapeutic strategies and future prospects. *Mol Cancer* 2020; **19**: 116.
56. Gavin MA, Torgerson TR, Houston E *et al*. Single-cell analysis of normal and FOXP3-mutant human T cells: FOXP3 expression without regulatory T cell development. *Proc Natl Acad Sci USA* 2006; **103**: 6659–6664.
57. Allan SE, Crome SQ, Crellin NK *et al*. Activation-induced FOXP3 in human T effector cells does not suppress proliferation or cytokine production. *Int Immunol* 2007; **19**: 345–354.
58. Sainson RCA, Thotakura AK, Kosmac M *et al*. An antibody targeting ICOS increases Intratumoral cytotoxic to regulatory T-cell ratio and induces tumor regression. *Cancer Immunol Res* 2020; **8**: 1568–1582.
59. Ito T, Hanabuchi S, Wang Y-H *et al*. Two functional subsets of $FOXP3^+$ regulatory T cells in human thymus and periphery. *Immunity* 2008; **28**: 870–880.
60. Nakanishi J, Wada Y, Matsumoto K, Azuma M, Kikuchi K, Ueda S. Overexpression of B7-H1 (PD-L1) significantly associates with tumor grade and postoperative prognosis in human urothelial cancers. *Cancer Immunol Immunother* 2007; **56**: 1173–1182.
61. Wu C-T, Chen W-C, Chang Y-H, Lin W-Y, Chen M-F. The role of PD-L1 in the radiation response and clinical outcome for bladder cancer. *Sci Rep* 2016; **6**: e19740.
62. Eich M-L, Chaux A, Guner G *et al*. Tumor immune microenvironment in non–muscle-invasive urothelial carcinoma of the bladder. *Hum Pathol* 2019; **89**: 24–32.
63. Bellmunt J, Mullane SA, Werner L *et al*. Association of PD-L1 expression on tumor-infiltrating mononuclear cells and overall survival in patients with urothelial carcinoma. *Ann Oncol* 2015; **26**: 812–817.
64. Roche. VENTANA PD-L1 (SP142) Assay Interpretation Guide for Urothelial Carcinoma. 2020.
65. Eckstein M, Erben P, Kriegmair MC *et al*. Performance of the Food and Drug Administration/EMA-approved programmed cell death ligand-1 assays in urothelial carcinoma with emphasis on therapy stratification for first-line use of atezolizumab and pembrolizumab. *Eur J Cancer* 2019; **106**: 234–243.
66. Rijnders M, van der Veldt AAM, Zuiverloon TCM *et al*. PD-L1 antibody comparison in urothelial carcinoma. *Eur Urol* 2019; **75**: 538–540.
67. Bellmunt J, de Wit R, Vaughn DJ *et al*. Pembrolizumab as second-line therapy for advanced urothelial carcinoma. *N Engl J Med* 2017; **376**: 1015–1026.
68. Balar AV, Castellano D, O'Donnell PH *et al*. First-line pembrolizumab in cisplatin-ineligible patients with locally advanced and unresectable or metastatic urothelial cancer (KEYNOTE-052): a multicentre, single-arm, phase 2 study. *Lancet Oncol* 2017; **18**: 1483–1492.
69. Powles T, Durán I, van der Heijden MS *et al*. Atezolizumab versus chemotherapy in patients with platinum-treated locally advanced or metastatic urothelial carcinoma (IMvigor211): a multicentre, open-label, phase 3 randomised controlled trial. *Lancet* 2018; **391**: 748–757.

70. Kamoun A, de Reyniès A, Allory Y *et al*. A consensus molecular classification of muscle-invasive bladder cancer. *Eur Urol* 2020; **77**: 420–433.
71. Guo CC, Bondaruk J, Yao H *et al*. Assessment of luminal and basal phenotypes in bladder cancer. *Sci Rep* 2020; **10**, 9743.
72. Lindskrog SV, Prip F, Lamy P *et al*. An integrated multi-omics analysis identifies prognostic molecular subtypes of non-muscle-invasive bladder cancer. *Nat Commun* 2021; **12**: 23–31.
73. Lobo J, Monteiro-Reis S, Guimarães-Teixeira C *et al*. Practicability of clinical application of bladder cancer molecular classification and additional value of epithelial-to-mesenchymal transition: prognostic value of vimentin expression. *J Transl Med* 2020; **18**: 303.
74. Lv J, Zhu Y, Ji A, Zhang Q, Liao G. Mining TCGA database for tumor mutation burden and their clinical significance in bladder cancer. *Biosci Rep* 2020; **40**: BSR20194337.
75. Hodgson A, Vesprini D, Liu SK, Xu B, Downes MR. Correlation of mismatch repair protein deficiency, PD-L1 and CD8 expression in high-grade urothelial carcinoma of the bladder. *J Clin Pathol* 2020; **73**: 519–522.
76. Amin MB, Edge S, Greene F *et al*. *AJCC Cancer Staging Manual*. 8th ed. Berlin: Springer; 2017.

Supporting Information

Additional supporting information may be found online in the Supporting Information section at the end of the article.

Graphical Abstract

The contents of this page will be used as part of the graphical abstract of html only. It will not be published as part of main.

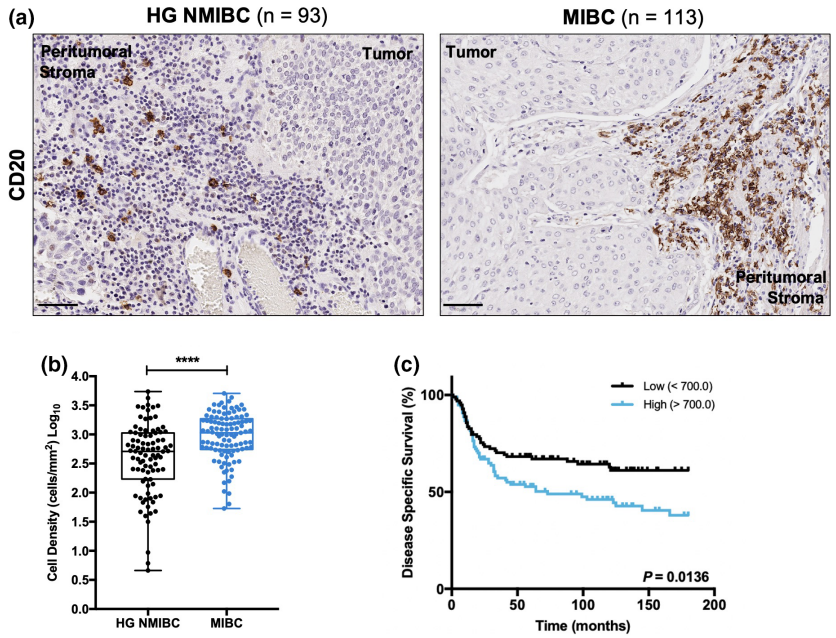

In this study, we characterised and compared the immune infiltrate of two subtypes of bladder cancer (BICa): high-grade-non-muscle invasive BICa (HG NMIBC) and muscle-invasive BICa (MIBA). A total of 206 tissue samples were immunohistochemically stained for ten immune biomarkers, and positive staining was quantified using a digital pathology software, what granted a more precise and reproducible analysis, besides allowing for workflow customisation (education of adequate algorithms). Immune infiltrates of HG NMIBC and MIBC were found to display significant differences that may help selecting patients for treatment with immunotherapies. Moreover, ICOS, a costimulatory immune checkpoint, was identified as a potential therapeutic target for certain BICa patient subsets.